The Joint-limits and Singularity Avoidance in Robotic Welding

Liguo Huo [a] and Luc Baron [b]

[a] *Department of Mechanical Engineering*
École Polytechnique de Montréal
P.O. 6079, station Centre-Ville
Montréal, Québec, Canada, H3C 3A7
liguo.huo@polymtl.ca
[b] *Department of Mechanical Engineering*
École Polytechnique de Montréal
P.O. 6079, station Centre-Ville
Montréal, Québec, Canada, H3C 3A7
luc.baron@polymtl.ca

Abstract

Purpose: The aim of this research is to develop a redundancy-resolution (RR) algorithm to optimize the joint space trajectory of the six-rotation-axis industrial robot as performing arc-welding tasks.

Design/methodology/approach: The rotation of the tool around its symmetry axis is clearly irrelevant to the view of the task to be accomplished besides some exceptional situations. When performed with a general 6-DOF manipulator, there exists one DOF of redundancy that remains. By taking advantage of the symmetry axis of the welding electrode, we decompose the required instantaneous twist of the electrode into two orthogonal components, one lying into the relevant task subspace and one into the redundant task subspace, respectively. Joint-limits and singularity avoidance are considered as the optimization objectives.

Finding: The twist-decomposition algorithm is able to optimize effectively the joint space trajectory. It has been tested and demonstrated in simulation.

Originality/value: A new RR algorithm is introduced for the 6-rotation-axis industrial robot performing welding tasks. A new kinetostatic performance index is proposed on evaluating the kinematic quality of robotic postures. It can also be used in other applications like milling, deburing and many other tasks requiring less than six-DOF in tool frame.

1. Introduction

The inverse kinematics of serial robotic manipulators has been in-depth studied for decades at both displacement and velocity levels. It is well known that the former is highly nonlinear and deserve dedicated solution procedures, while the latter is linear and requires the inversion of the Jacobian matrix of the manipulator. For a general 6-*degrees-of-freedom* (DOF) task, many research works have reported algorithms (e.g., Liégeois, 1977; Siciliano, 1992; Yoshikawa, 1996; Whitney, 1972; Klein and Huang, 1983; Angeles *et al.*, 1987; Arenson *et al.*, 1998; Baron, 2000) allowing to choose an optimal solution when the manipulator has more joints than the corresponding DOF of its *end-effector* (EE). All of them use the *Gradient Projection Method* (GPM) to track the desired EE path, *i.e.*, the main task, and solve a trajectory optimization problem, *i.e.*, the secondary task. The latter is related to a performance criterion. The gradient of this function is projected onto the null space of the Jacobian matrix, namely $\mathbf{J}$, in order to choose the best solution among the infinitely many that exist. Hence, the secondary task is performed under the constraint that the main task is realized.

The concept of *kinematic redundancy* is related to the definition of the task instead of being only an intrinsic property of the manipulator. Although this fact is still not well understood in practice, it has been recognized by several researchers. Samson *et al.* (1991) clearly presented that the redundancy depends on the task and may change with time. Sciavicco and Siciliano (2000) said that the manipulator can be *functionally redundant* when only a number of components of its operational space are concerned with a specific task, even if the dimension of operational and joint spaces are equal. Although Siciliano proposed the concept of functional redundancy, he didn't develop the corresponding solution procedure.

In the case of functional redundancy, $\mathbf{J}$ is often a full rank square matrix, *i.e.*, its null space doesn't exist, thus the general projection method working on the null space of $\mathbf{J}$ can not be applied here. In fact, there are many industrial tasks such as welding and many other tasks like milling, deburing, laser-cutting and gluing, that require less than six-DOF, because of the presence of a symmetry axis or plane in the

operation. For example, the general arc-welding task requires 3-DOF for the displacement of the end-point of the electrode, but requires only 2-DOF for the orientation of the electrode axis. The rotation of the welding-tool around the electrode symmetry axis is clearly irrelevant to the view of the task to be accomplished, the so-called functional redundancy. Baron (2000) proposed to add a virtual joint to the manipulator so that a column is added to $\mathbf{J}$, thus rendering it underdetermined. This *augmented approach* in solving functional redundancy suffers from the potential ill-conditioning of the augmented $\mathbf{J}$, and the additional computation cost required to solve this augmented $\mathbf{J}$. Alternatively, Huo and Baron (2005) proposed the *twist decomposition approach* (TWA) to solve the functional redundancy. Instead of using the projection onto the null space of $\mathbf{J}$, the TWA is based on the orthogonal decomposition of the required twist into two orthogonal subspaces in the instantaneous tool frame. The TWA has great difference with the *task-decomposition approach* proposed by Nakamura *et al.* (1987) on the theoretical base, although both of them consider the order of task priority. First, the TWA classifies the order of task priority in the instantaneous tool frame instead of in the robot base frame. Second, the TWA is directly developed from the minimum-norm solution without considering the projection onto the null space of $\mathbf{J}$, while the development of the task-decomposition approach is based on the general equation using the null space of $\mathbf{J}$.

Chaumette and Marchand (2001) have realized that the success of the GPM relies on the evaluation of the performance criterion on the joints position. As the task requires not only the avoidance of the joint-limits but also keeping the robot configuration as far as possible from singularities, we need two different performance criterions relating to joint-limits and singularities, respectively. Here, the distance to the mid-joint position is used as the performance index relating to the joint-limits. A new performance index relating to singularities, named *Parameter of Singularity*, is proposed by combining the *Manipulability Measure*, proposed by Yoshikawa (1984), and the *condition number* of $\mathbf{J}$, first used by Salisbury and Craig (1982).

In this paper, the solutions for the two kinds of redundancy, *i.e.*, intrinsic and functional redundancy, are reviewed, particularly the TWA for the functional redundancy. Finally, a numerical example with application to arc-welding is demonstrated.

2. Background on Kinematic Redundancy

Before formulating the problem, let us briefly recall the two basic sources of kinematic redundancy of a robotic manipulator with respect to a given task.

2.1. *Basic Definitions*

Let $\mathcal{J}$ denote, the *joint space* of a robotic manipulator having $n+1$ rigid bodies serially connected by n joints, either revolute R or prismatic P. The posture of the manipulator in $\mathcal{J}$ is given by the n-dimensional vector, namely $\boldsymbol{\theta}$, and hence, $n = \dim(\mathcal{J}) = \dim(\boldsymbol{\theta})$.

Moreover, let $\mathcal{O}$ denote, the *operational space* of the EE of the robotic manipulator resulting from the joint space $\mathcal{J}$. Since any free-moving rigid body in space can have at most six DOFs, the dimension of $\mathcal{O}$ is also at most six, and hence, $o = \dim(\mathcal{O}) \leq 6$.

Furthermore, let $\mathcal{T}$ denote, the *task space* such as required by the functional mobility of the EE, independently of the manipulator's architecture and hence, $t = \dim(\mathcal{T}) \leq 6$. Now, let us recall the following three definitions:

Definition 1: Intrinsic redundancy
A serial manipulator is said to be intrinsically redundant when the dimension of the joint space $\mathcal{J}$, denoted by $n = \dim(\mathcal{J})$, is greater than the dimension of the resulting operational space $\mathcal{O}$ of the EE, denoted by $o = \dim(\mathcal{O}) \leq 6$, i.e.*, when $n > o$. The degree of intrinsic redundancy of a serial manipulator, namely r_I, is computed as*

$$r_I = n - o. \tag{1}$$

Definition 2: Functional redundancy *
A pair of serial manipulator-task is said to be functionally redundant when the dimension of the operational space $\mathcal{O}$ of the EE, denoted by $o = \dim(\mathcal{O}) \leq 6$, is greater than the dimension of the task space $\mathcal{T}$ of the EE, denoted by $t = \dim(\mathcal{T}) \leq 6$, while the task space being totally included into the operation space of the manipulator, i.e.*, $\mathcal{T} \subseteq \mathcal{O}$, and hence, $o > t$. The degree of functional redundancy of a pair of serial manipulator-task, namely r_F, is computed as*

$$r_F = o - t. \tag{2}$$

* This definition of functional redundancy of serial manipulator-task is expandable to other types of manipulators such as parallel and hybrid ones.

Definition 3: Kinematic redundancy
A pair of serial manipulator-task is said to be kinematically redundant when the dimension of the joint space $\mathcal{J}$, denoted by $n = \dim(\mathcal{J})$, is greater than the dimension of the task space $\mathcal{T}$ of the EE, denoted by $t = \dim(\mathcal{T}) \leq 6$, while the task space being totally included into the resulting operation space of the manipulator, i.e.*, $\mathcal{T} \subseteq \mathcal{O}$, and hence, $n > t$. The degree of kinematic redundancy of a pair of serial manipulator-task, namely r_K, is computed as*

$$r_K = n - t. \tag{3}$$

Upon substitution of eqs.(1) and (2) into eq.(3), it becomes apparent that the kinematic redundancy come from two sources, the intrinsic and functional redundancies, *i.e.*,

$$r_K = r_I + r_F. \tag{4}$$

In the literature, most of the research working on redundancy-resolution of serial manipulators suppose that $r_F = 0$, and thus, study $r_K = r_I$. In this paper, the opposite case is studied, *i.e.*, supposing $r_I = 0$, and thus, study $r_K = r_F$.

2.2. *Problem Formulation*

The inverse kinematics of serial manipulators is usually based on the linear relationship between the EE velocity, called *twist* and denoted $\mathbf{t}$, and the joint velocities, denoted $\dot{\boldsymbol{\theta}}$, given by

$$\mathbf{t} = \mathbf{J}\dot{\boldsymbol{\theta}}, \tag{5}$$

with $\mathbf{t}$ and $\dot{\boldsymbol{\theta}}$ defined as

$$\mathbf{t} \equiv [\boldsymbol{\omega}^T \dot{\mathbf{p}}^T]^T \in 2 \times \Re^3, \quad \dot{\boldsymbol{\theta}} \equiv [\dot{\theta}_1 \cdots \dot{\theta}_n]^T \in \Re^n, \tag{6}$$

and the Jacobian matrix $\mathbf{J}$ being defined as

$$\mathbf{J} \equiv \begin{bmatrix} \mathbf{A} \\ \mathbf{B} \end{bmatrix}, \quad \mathbf{A}, \mathbf{B} \in \Re^{3 \times n}, \tag{7}$$

where $\boldsymbol{\omega} \in \Re^3$ is the angular velocity vector of the EE, $\dot{\mathbf{p}} \in \Re^3$ is the translation velocity vector of a point on the EE, while $\dot{\theta}_i$ is the velocity of joint i. It is noteworthy that $\mathbf{t}$ is not defined as a vector of $\Re^6$, but rather as a set of two vectors of $\Re^3$ casted into a column array, and hence, $\mathbf{t} \in 2 \times \Re^3 \neq \Re^6$. This distinction is important and will be further used in section 3. For the sake of numerical computation, we replace velocities by small displacements in eq.(5), *i.e.*, $\mathbf{t} \rightarrow \boldsymbol{\Delta}\mathbf{t}$ and $\dot{\boldsymbol{\theta}} \rightarrow \boldsymbol{\Delta\theta}$.

• When $\mathbf{J}$ is square:

The resolved motion-rate method proposed by Whitney (1969) can be used to compute $\boldsymbol{\Delta\theta}$ as

$$\boldsymbol{\Delta\theta} = \mathbf{J}^{-1}\boldsymbol{\Delta}\mathbf{t}, \tag{8}$$

where it is apparent that $\mathbf{J}$ must be non-singular.

• When $\mathbf{J}$ has more rows than columns:

The mobility of the EE is less than 6-DOF, because the manipulator has either less than six joints and/or these joints do not allow to produce the full EE mobility. In both cases, the $\boldsymbol{\Delta\theta}$ can be computed from $\boldsymbol{\Delta}\mathbf{t}$ as

$$\boldsymbol{\Delta\theta} = \mathbf{J}^*\boldsymbol{\Delta}\mathbf{t}, \tag{9}$$

where $\mathbf{J}^*$ is the left generalized inverse of $\mathbf{J}$ such that

$$\mathbf{J}^* \equiv (\mathbf{J}^T\mathbf{J})^{-1}\mathbf{J}^T. \tag{10}$$

This left generalized inverse is usually not required, because there always exist a time-invariant frame in which the constrained mobility of the EE are rows of zeros in $\mathbf{J}$. Thus, the user can directly eliminate these rows from $\mathbf{J}$ in order to render it square and full rank. For example, planar and spherical serial manipulators belong to this case.

• When $\mathbf{J}$ has less rows than columns:

For intrinsically-redundant serial manipulators, $\mathbf{J}$ always has more columns than rows, and hence, eq.(5) becomes an underdetermined linear algebraic system having infinitely many solutions. In this case, Liégeois (1977) proposed to compute $\boldsymbol{\Delta\theta}$ as

$$\boldsymbol{\Delta\theta} = \underbrace{(\mathbf{J}^\dagger)\boldsymbol{\Delta}\mathbf{t}}_{\text{minimum-norm solution}} + \underbrace{(\mathbf{1} - \mathbf{J}^\dagger\mathbf{J})\mathbf{h}}_{\text{homogeneous solution}}, \tag{11}$$

where $\mathbf{J}^\dagger$ is defined as the right generalized inverse of $\mathbf{J}$ such that

$$\mathbf{J}^\dagger \equiv \mathbf{J}^T(\mathbf{J}\mathbf{J}^T)^{-1}, \tag{12}$$

and $\mathbf{h}$ is an arbitrary vector of $\mathcal{J}$ allowing to satisfy a secondary task. The first term in the right-hand side (RHS) of eq.(11) is known as the minimum-norm solution of eq.(5), *i.e.*, the $\boldsymbol{\Delta\theta}_M$ that minimizes $\|\boldsymbol{\Delta\theta}\|$ among all the $\boldsymbol{\Delta\theta}$ that are solutions of eq.(5). The second part of the RHS of eq.(11) is known as the homogeneous solution of eq.(5), *i.e.*, the $\boldsymbol{\Delta\theta}_H$ that produce $\boldsymbol{\Delta}\mathbf{t} = \mathbf{0}$, *i.e.*, no displacement of the EE. This joint displacement $\boldsymbol{\Delta\theta}_H$ is also known as the

self-motion of the manipulator. It is symbolically computed as the projection of an arbitrary vector $\mathbf{h}$ onto the null space of $\mathbf{J}$ with the orthogonal projector $(\mathbf{1} - \mathbf{J}^{\dagger}\mathbf{J})$. Equation (11) is used to solve the kinematic inversion of intrinsically-redundant manipulators by many researchers, *e.g.*, Siciliano (1992) and Yoshikawa (1996), including Arenson *et al.* (1998) who payed a special attention in avoiding the squaring of the condition number while solving eq.(11).

Sometimes, it exists a time-invariant frame in which the functional redundancy are rows of $\mathbf{J}$. In this case, the eq.(11) can be used to solve the inverse kinematics with these rows previously eliminated from $\mathbf{J}$. For example, an arc-welding task may require the 3-D positioning of the end-point of the welding electrode as keeping the electrode axis always parallel with one axis of the base frame. In this case, the redundant task is the orientation around the electrode axis, *e.g.*, the vertical axis, which is time-invariant in the base frame. Most of the times, it is not possible to find such a time-invariant frame to express the functional redundancy of a task. For general arc-welding, the electrode axis needs to undergo arbitrary orientations in space, and hence, the electrode axis is time-varying in base frame. Therefore, eq.(11) can not be used. Below, a TWA on solving this problem is compared with the augmented approach.

3. Twist-Decomposition Approach

Before proposing a functional-redundancy resolution algorithm, let us briefly review the orthogonal decomposition of vectors and twists.

3.1. *Orthogonal-Decomposition of Vectors*

Decomposing any vector $(\,\cdot\,)$ of $\Re^3$ into two orthogonal parts, $[\,\cdot\,]_M$, the component lying in the subspace, $\mathcal{M}$, and $[\,\cdot\,]_{M^\perp}$, the component lying in the orthogonal subspace, $\mathcal{M}^\perp$, using the *projector* $\mathbf{M}$ and an *orthogonal complement* of $\mathbf{M}$, namely $\mathbf{M}^\perp$, as follows:

$$(\,\cdot\,) = [\,\cdot\,]_M + [\,\cdot\,]_{M^\perp} = \mathbf{M}(\,\cdot\,) + \mathbf{M}^\perp(\,\cdot\,). \tag{13}$$

It is apparent from eq.(13), that $\mathbf{M}$ and $\mathbf{M}^\perp$ are related by $\mathbf{M} + \mathbf{M}^\perp = \mathbf{1}$ and $\mathbf{M}\mathbf{M}^\perp = \mathbf{O}$, where $\mathbf{1}$ and $\mathbf{O}$ are the 3×3 identity and zero matrices, respectively. The orthogonal complement of $\mathbf{M}$ thus defined, $\mathbf{M}^\perp$, is therefore unique. The projector $\mathbf{M}$ projects vectors of $\Re^3$ onto the subspace $\mathcal{M}$, while the orthogonal projector $\mathbf{M}^\perp$ projects those vectors onto the orthogonal subspace $\mathcal{M}^\perp$. These projectors are given for the four possible dimensions i of subspaces of $\Re^3$ as:

$$\mathbf{M}_i = \begin{cases} \mathbf{1} \\ \mathbf{P} \\ \mathbf{L} \\ \mathbf{O} \end{cases}, \mathbf{M}_i^\perp = \begin{cases} \mathbf{O} & i = 3 \Rightarrow \text{3-D task} \\ \mathbf{L} & i = 2 \Rightarrow \text{2-D task} \\ \mathbf{P} & i = 1 \Rightarrow \text{1-D task} \\ \mathbf{1} & i = 0 \Rightarrow \text{0-D task} \end{cases}, \tag{14}$$

where the plane and line projectors, $\mathbf{P}$ and $\mathbf{L}$, respectively, are defined as:

$$\mathbf{P} \equiv \mathbf{1} - \mathbf{L}, \quad \mathbf{L} \equiv \mathbf{e}\mathbf{e}^T, \tag{15}$$

in which $\mathbf{e}$ is a unit vector along the line $\mathcal{L}$ and normal to the plane $\mathcal{P}$. The null-projector $\mathbf{O}$ is the 3×3 zero matrix that projects any vector of $\Re^3$ onto the null-subspace $\mathcal{O}$, while the identity-projector $\mathbf{1}$ is the 3×3 identity matrix that projects any vector of $\Re^3$ onto itself.

3.2. *Orthogonal-Decomposition of Twists*

Any twist array $(\,\cdot\,)$ of $2 \times \Re^3$ can also be decomposed into two orthogonal parts, $[\,\cdot\,]_{\mathcal{T}}$, the component lying on the task subspace, $\mathcal{T}$, and $[\,\cdot\,]_{\mathcal{T}^\perp}$, the component lying on the orthogonal task subspace (also designated as the redundant subspace), $\mathcal{T}^\perp$, using the *twist projector* $\mathbf{T}$ and an *orthogonal complement* of $\mathbf{T}$, namely $\mathbf{T}^\perp$, as follows:

$$(\,\cdot\,) = [\,\cdot\,]_{\mathcal{T}} + [\,\cdot\,]_{\mathcal{T}^\perp} = \mathbf{T}(\,\cdot\,) + \mathbf{T}^\perp(\,\cdot\,) \tag{16}$$

It is apparent from eq.(16), that $\mathbf{T}$ and $\mathbf{T}^\perp$ are projectors of twists that must verify all the properties of projectors reviewed before. However, twists are not vectors of $\Re^6$, and hence, projectors of twists cannot be defined as in eqs.(14) and (15), *e.g.*,

$$\mathbf{T} \neq \mathbf{t}\mathbf{t}^T, \quad \mathbf{T}^\perp \neq \mathbf{1} - \mathbf{t}\mathbf{t}^T, \tag{17}$$

but must rather be defined as block diagonal matrices of projectors of $\Re^3$, *i.e.*,

$$\mathbf{T} \equiv \begin{bmatrix} \mathbf{M}_\omega & \mathbf{O} \\ \mathbf{O} & \mathbf{M}_v \end{bmatrix}, \tag{18}$$

$$\mathbf{T}^\perp \equiv \mathbf{1} - \mathbf{T} = \begin{bmatrix} \mathbf{1} - \mathbf{M}_\omega & \mathbf{O} \\ \mathbf{O} & \mathbf{1} - \mathbf{M}_v \end{bmatrix}, \tag{19}$$

where $\mathbf{M}_\omega$ and $\mathbf{M}_v$ are projectors of $\Re^3$ defined in eqs.(14) and (15) which allow the projection of the angular and translational velocity vectors, respectively. It is noteworthy that the matrices of eq.(17) do not verify the properties of projectors, and hence, can not be used for orthogonal decomposition. Finally, eq.(16) becomes

$$\mathbf{t} = \mathbf{t}_{\mathcal{T}} + \mathbf{t}_{\mathcal{T}^\perp} = \mathbf{T}\mathbf{t} + (\mathbf{1} - \mathbf{T})\mathbf{t}. \tag{20}$$

3.3. *Functional-Redundancy Resolution*

For functionally-redundant serial manipulators, it is possible to decompose the twist of the EE into two orthogonal parts, one lying into the task subspace and another one lying into the redundant subspace. Substituting eq.(20) into eq.(8) yields

$$\boldsymbol{\Delta\theta} = \underbrace{(\mathbf{J}^\dagger\mathbf{T})\boldsymbol{\Delta}\mathbf{t}}_{\text{task displacement}} + \underbrace{\mathbf{J}^\dagger(\mathbf{1} - \mathbf{T})\mathbf{J}\mathbf{h}}_{\text{redundant displacement}}, \tag{21}$$

where $\mathbf{h}$ is an arbitrary vector of $\mathcal{J}$ allowing to satisfy a secondary task, and is often chosen as the gradient of a performance criterion function to be minimized.

The first part of the RHS of eq.(21) is the joint displacement required by the task, while the second part is the joint displacement in the redundant subspace (or irrelevant to the task). Clearly, eq.(21) does not require the projection onto the null-space of $\mathbf{J}$ as most of the redundancy-resolution algorithms do, but rather requires an orthogonal projection based on the instantaneous geometry of the task to be accomplished. As shown in Algorithm I, eq.(21) is used within a resolved-motion rate method. At lines 1-3, the joint position $\boldsymbol{\theta}$ and the desired EE pose $\{\mathbf{p}_d, \mathbf{Q}_d\}$ are first initialized, then the actual EE pose $\{\mathbf{p}, \mathbf{Q}\}$ is computed with the direct kinematic model $\mathbf{DK}(\boldsymbol{\theta})$. At lines 4-6, an EE displacement $\Delta\mathbf{t}$ is computed from the difference between the desired and actual EE poses. The $\mathbf{vect}(\,\cdot\,)$ at line 6 is the function transforming a 3×3 rotation matrix into an axial vector as defined in Angeles (2003) (page 34). At lines 7-8, the instantaneous orthogonal twist projector $\mathbf{T}$ is computed from $\mathbf{DK}(\boldsymbol{\theta})$. At line 9, the orthogonal decomposition method is used to compute the corresponding joint displacement $\Delta\boldsymbol{\theta}$. Finally, the algorithm is stop whenever the norm of $\Delta\boldsymbol{\theta}$ is smaller than a certain threshold ϵ.

Algorithm I: Twist-Decomposition Algorithm

1 $\boldsymbol{\theta} \longleftarrow$ initial joint position;
2 $\{\mathbf{p}_d, \mathbf{Q}_d\} \longleftarrow$ desired EE pose;
3 $\{\mathbf{p}, \mathbf{Q}\} \Leftarrow \mathbf{DK}(\boldsymbol{\theta})$
4 $\Delta\mathbf{Q} \Leftarrow \mathbf{Q}^T\mathbf{Q}_d$
5 $\Delta\mathbf{p} \Leftarrow \mathbf{p}_d - \mathbf{p}$
6 $\Delta\mathbf{t} \leftarrow \begin{bmatrix} \mathbf{Qvect}(\Delta\mathbf{Q}) \\ \Delta\mathbf{p} \end{bmatrix}$
7 $\mathbf{DK}(\boldsymbol{\theta}) \Rightarrow \quad \mathbf{e} \Rightarrow \mathbf{M}_\omega, \quad \mathbf{f} \Rightarrow \mathbf{M}_v, \quad \mathbf{J}$
8 $\mathbf{T} \Leftarrow \begin{bmatrix} \mathbf{M}_\omega & \mathbf{O} \\ \mathbf{O} & \mathbf{M}_v \end{bmatrix}$,
9 $\Delta\boldsymbol{\theta} \Leftarrow \mathbf{J}^\dagger\mathbf{T}\Delta\mathbf{t} + \mathbf{J}^\dagger(\mathbf{1} - \mathbf{T})\mathbf{J}\mathbf{h}$
10 if $\|\Delta\boldsymbol{\theta}\| < \epsilon$ then stop;
else
11 $\boldsymbol{\theta} \Leftarrow \boldsymbol{\theta} + \Delta\boldsymbol{\theta}$, and go to 3.

4. Performance Criterions

4.1. *Joint-limits Avoidance*

While performing the joint-limits avoidance as the secondary task, we would like to keep the manipulator as far as possible from its joint limits. Thus, in the case of avoidance of the joint-limits (Baron, 2000; Huo and Baron, 2005), the performance criterion can be written as to maintain the manipulator as close as possible to the mid-joint position $\bar{\boldsymbol{\theta}}$, *i.e.*,

$$z_{joint} = \frac{1}{2}(\boldsymbol{\theta} - \bar{\boldsymbol{\theta}})^T\mathbf{W}^T\mathbf{W}(\boldsymbol{\theta} - \bar{\boldsymbol{\theta}}) \rightarrow \min_{\boldsymbol{\theta}}, \tag{22}$$

with $\bar{\boldsymbol{\theta}}$ and $\mathbf{W}$ being defined as

$$\bar{\boldsymbol{\theta}} \equiv \frac{1}{2}(\boldsymbol{\theta}_{max} + \boldsymbol{\theta}_{min}), \quad \mathbf{W} \equiv \mathbf{Diag}(\mathbf{w}). \tag{23}$$

The setting of the weighting vector $\mathbf{w}$ of eq.(23) is very important for the success. If $\mathbf{w}$ is too small, the redundant displacement may not be sufficient to avoid the joint-limits; if $\mathbf{w}$ is too large, the redundant displacement may produce high joint velocities. Therefore, $\mathbf{w}$ is usually set based on trial and error.

4.2. *Kinematic Singularity Avoidance*

A singular posture is defined as the manipulator's configuration $\boldsymbol{\theta}^*$, where $\mathbf{J}(\boldsymbol{\theta}^*)$ is not full rank. The Singular Value Decomposition (SVD) of $\mathbf{J}$ is

$$\mathbf{J} = \mathbf{U}\boldsymbol{\Sigma}\mathbf{V}^T, \quad \boldsymbol{\Sigma} \equiv \mathbf{Diag}(\sigma_1, \cdots, \sigma_m), \tag{24}$$

where $\mathbf{U}$ and $\mathbf{V}$ are, respectively, $m \times m$ and $n \times n$ orthogonal matrices, and $\boldsymbol{\Sigma}$ is an $m \times n$ diagonal matrix of the singular values of $\mathbf{J}$. The manipulator is in a singular state when at least one of its singular value equal to zero, *i.e.*, $\sigma_i = 0$. The corresponding column of $\mathbf{U}$, $\mathbf{u}_i$ is referred to as the singular direction s. In this state, the motion along the singular directions is not possible (Bedrossian, 1990).

Moreover, in the neighborhood of singular points, even a small change in $\boldsymbol{\Delta}\mathbf{t}$ requires an enormous change in $\boldsymbol{\Delta\theta}$, which is not-practically feasible and dangerous in real manipulators.

4.2.1. *Manipulability*

The first step in avoiding singularities is to detect them in the joint space. As presented by Yoshikawa (1990), the *manipulability ellipsoid* represents an ability of manipulation, *i.e.*, the EE can move at higher speed in the direction of the major axis of the ellipsoid, while only with lower speed in the direction of the minor axes. If the ellipsoid is a sphere, the EE can move in all directions uniformly. Moreover, the larger the volume of the ellipsoid is, the faster the EE can move. One of the representative measures for the ability of manipulation derived from the manipulability ellipsoid is the volume of the ellipsoid. Hence, the measure of manipulability, namely ω_{mom}, could be written as

$$\omega_{mom} = \sqrt{det(\mathbf{J}\mathbf{J}^T)} = \sigma_1\sigma_2\cdots\sigma_m. \tag{25}$$

where $\sigma_1,\ \sigma_2,\ \cdots\sigma_m$ are the singular values of $\mathbf{J}$ ordered from maximum to minimum.

Thus, let the $\mathbf{u}_i$ be the ith column vector of $\mathbf{U}$, the principle axes of the manipulability ellipsoid are $\sigma_1\mathbf{u}_1$, $\sigma_2\mathbf{u}_2$, ..., $\sigma_m\mathbf{u}_m$ (see Figure 1). Marani *et al.* (2002) have used the ω_{mom} as the distance criterion to avoid manipulator singularity.

4.2.2. *Conditioning*

Another index that might be induced from the manipulability ellipsoid is the *condition number*, namely

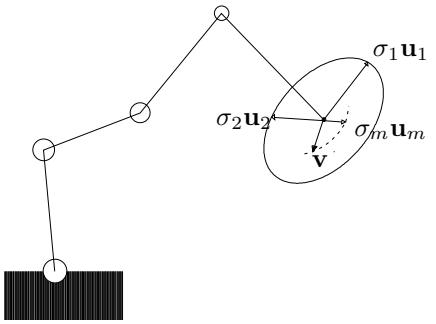

Figure 1. Representation of the manipulability ellipsoid

ω_{cond}, of $\mathbf{J}$, which is defined as the ratio of the maximum and minimum radius of the ellipsoid, *i.e.,*

$$\omega_{cond} = \frac{\sigma_1}{\sigma_m} \geq 1, \tag{26}$$

and is independent of the ellipsoid's size. This ratio is an index of the directional uniformly of the ellipsoid. The closer to unity this index is, the more spherical the ellipsoid is. In a singular posture, the minor axis of the ellipsoid vanishes, *i.e.*, $\sigma_m = 0$, so the condition number becomes infinity. The condition number can be used as the distance criterion to avoid manipulator's singularities.

4.2.3. *Parameter of Singularity*

We propose to combine the manipulability and conditioning together in order to generate a new performance index, named *Parameter of Singularity* (PS), and is defined as

$$\omega_{ps} \equiv \sqrt{\frac{\omega_{cond}}{\omega_{mom}}} = \sqrt{\frac{1}{\sigma_2\sigma_3\cdots\sigma_m^2}}. \tag{27}$$

The index ω_{ps} represents both the volume and the shape of the manipulability ellipsoid at the same time. The smaller ω_{ps} is, the more spherical the ellipsoid is or the larger the ellipsoid's volume is, the faster the EE can move in the direction of the minor axis. Thus, the ω_{ps} can be used as a continuous measure that evaluate the kinematic quality of a robotic posture. The greater the ω_{ps} is, the worse the conditioning is or the lower manipulability is.

When ω_{ps} is passing over a preset threshold value, the corresponding configuration at this instant is recorded as $\boldsymbol{\theta}_{Ts}$, and the performance criterion written as eq.(28) is activated to maintain the manipulator as close as possible to $\boldsymbol{\theta}_{Ts}$ in the following steps, until the ω_{ps} is lower than the preset threshold value, *i.e.*,

$$z_{sing} = \frac{\omega_{ps}^2}{2}(\boldsymbol{\theta} - \boldsymbol{\theta}_{Ts})^T \mathbf{K}^T \mathbf{K}(\boldsymbol{\theta} - \boldsymbol{\theta}_{Ts}) \rightarrow \min_{\boldsymbol{\theta}}, \quad (28)$$

where $\mathbf{K}$ is a weighting matrix obtained with the same method as $\mathbf{W}$.

4.3. *Joint-limits and Kinematic Singularity Avoidance*

The two secondary tasks described above, joint-limits and kinematic singularity avoidances, can be combined into an unique performance criterion, which is to maintain the manipulator as close as possible to the mid-joint position $\bar{\boldsymbol{\theta}}$ and as far as possible to the singularities at the same time. The objective function could be written as

$$z = z_{joint} + z_{sing}. \quad (29)$$

By tuning $\mathbf{W}$ and $\mathbf{K}$, the relative importance between the two sub-tasks is adjusted. Vector $\mathbf{h}$ of eqs.(11, 21) is thus chosen as minus the gradient of z, *i.e.*,

$$\mathbf{h} = -\boldsymbol{\nabla} z = \mathbf{W}(\bar{\boldsymbol{\theta}} - \boldsymbol{\theta}) + \mathbf{K}\omega_{ps}(\boldsymbol{\theta}_{Ts} - \boldsymbol{\theta}). \quad (30)$$

5. Robotic Welding Example

When performing arc-welding operations, the electrode of the welding tool has a symmetry axis around which the welding tool may be rotated without interfering with the task. This axis describes the geometry of the functional redundancy (or the redundant subspace of twists). The unit vector $\mathbf{e}$ denote the orientation of the symmetry axis along the electrode. The projection of $\boldsymbol{\omega}$ along $\mathbf{e}$ is the irrelevant component of $\boldsymbol{\omega}$, while its projection onto the plane normal to $\mathbf{e}$ is the relevant component of $\boldsymbol{\omega}$. For an arc-welding task, the twist projectors are defined as

$$\mathbf{T}_{weld} \equiv \begin{bmatrix} (\mathbf{1} - \mathbf{e}\mathbf{e}^T) & \mathbf{0} \\ \mathbf{0} & 1 \end{bmatrix}, \quad \mathbf{T}_{weld}^{\perp} \equiv \begin{bmatrix} \mathbf{e}\mathbf{e}^T & \mathbf{0} \\ \mathbf{0} & 0 \end{bmatrix}. \quad (31)$$

Now, substituting eq.(31) into eq.(21) yields

$$\boldsymbol{\Delta\theta} = \mathbf{J}^{\dagger}\mathbf{T}_{weld}\Delta\mathbf{t} + \mathbf{J}^{\dagger} \begin{bmatrix} \mathbf{e}\mathbf{e}^T\mathbf{A}\mathbf{h} \\ \mathbf{0} \end{bmatrix}, \quad (32)$$

where $\mathbf{A}$ is the upper three rows of $\mathbf{J}$ as defined in eq.(6). Equation (32) can be used as line 9 of Algorithm I in order to solve the inverse kinematics of serial manipulators while performing an arc-welding task.

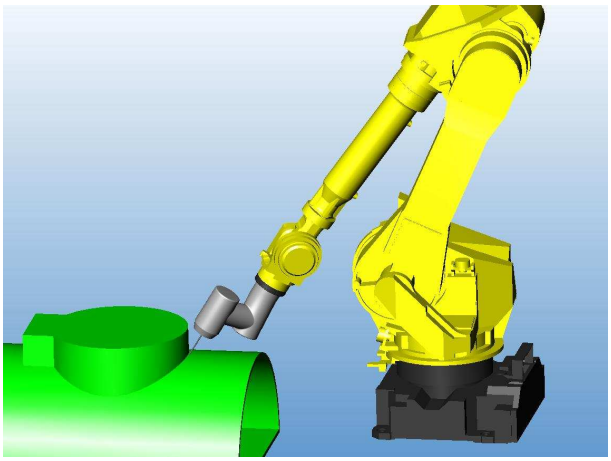

Figure 2. Graphic simulator of arc-welding operation with a Fanuc M-710 iC/50 .

5.1. *Task Description*

The arc-welding operation is performed with a Fanuc M-710 iC/50. The Denavit-Hartenberg (DH) parameters and joint limits of this robot are described in Table 1. The welding parts is made of two cylinder of radius 400mm and 250mm, respectively. Figure 2 shows the robot and the welding parts. The welding path Λ is the intersection curve of the two cylinders, as shown in Figure 3. The length of Λ is 1829mm. The EE must perform the welding operation consecutively along the path Λ, with the speed about 75mm/min. The welding tool symmetry axis must always be directed toward point P, which locates at $[\,0\ 0\ 0\,]$ in the part frame, the intersection point of the axes of the two cylinders. The transformation matrix from the robot base frame to the part frame is

Joint	θ_i	a_i	b_i	α_i	Max.	Min.
1	0	150	0	-90	180	-180
2	-90	870	0	180	75	-60
3	0	170	0	-90	230	-131.8
4	0	0	1016	90	360	-360
5	0	0	0	-90	125	-125
6	0	0	175	180	360	-360
unit	$degree$	mm	mm	$degree$	$degree$	$degree$

Table 1
DH parameters of Fanuc M-710ic/50

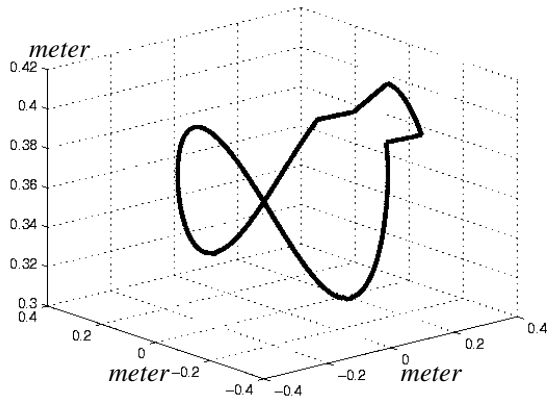

Figure 3. The welding path in the part frame.

$$\mathbf{T} = \begin{bmatrix} 1 & 0 & 0 & 1150 \\ 0 & 1 & 0 & 200 \\ 0 & 0 & 1 & -200 \\ 0 & 0 & 0 & 1 \end{bmatrix}. \tag{33}$$

Figure 4 shows the joint positions to perform twice the trajectory Λ as computed by the resolved-motion rate method without considering the functional redundancy, *i.e.*, using eq.(8) at line 9 of Algorithm I. Apparently, without taking advantage of the redundant axis, the sixth joint goes out of its joint limit, the manipulator is unable to perform this solution. Thus, an optimization is needed to avoid the joint-limits.

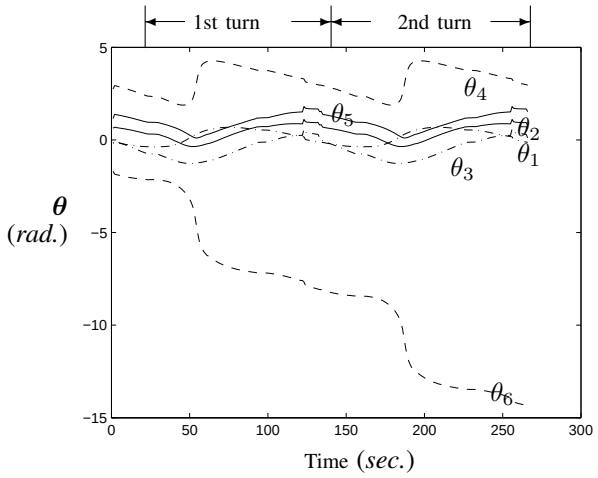

Figure 4. Joint positions of two consecutive turns of trajectory ¤ as computed by the resolved-motion rate method (without considering the functional redundancy).

5.2. *Test 1: Joint-limits Avoidance*

The secondary task $\mathbf{h}$ is chosen to avoid the joint-limits such that

$$\mathbf{h} = -\boldsymbol{\nabla} z_{joint} = \mathbf{Diag}(\mathbf{w}_{ini})(\bar{\boldsymbol{\theta}} - \boldsymbol{\theta}), \tag{34}$$

where $\bar{\boldsymbol{\theta}}$ is the mid-joint position of the robotic manipulator, and

$$\mathbf{w}_{ini} = \begin{bmatrix} 0.01 & 0.01 & 0.01 & 0.01 & 0.01 & 0.01 \end{bmatrix}. \tag{35}$$

Equation(34) is used as the secondary task to avoid the joint-limits. Figure 5 shows the joint positions for two consecutive turns as computed by the TWA, *i.e.*, using eq.(21) at line 9 of Algorithm I. The trajectories of each joint are within its joint limits. The maximum rotation velocity of fourth and sixth joints are 74.5 deg./s and 56.9 deg./s.

Although the TWA, with only joint limits avoidance, can reach a solution within the joint limits. The robot is close singularity at the instants 61 and 194 second, where the corresponding singularity performance indices are

$$\omega_{cond} = 163, \quad \omega_{mom} = 0.0066, \quad \omega_{ps} = 157. \tag{36}$$

Clearly, these indices are very close to a singularity. Thus, a singularity avoidance strategy becomes necessary in addition to the joint-limits avoidance for TWA.

5.3. *Test 2: Joint-limits and Kinematic Singularity Avoidance*

We can combine the two strategies as

$$z = z_{joint} + z_{sing} \rightarrow \min_{\boldsymbol{\theta}}, \tag{37}$$

and hence, the solution can be obtained as

$$\begin{aligned} \mathbf{h} &= -(\boldsymbol{\nabla} z_{joint} + \boldsymbol{\nabla} z_{sing}) \\ &= \mathbf{Diag}(\mathbf{w}_{ini})(\bar{\boldsymbol{\theta}} - \boldsymbol{\theta}) \\ &\quad + \mathbf{Diag}(\mathbf{k}_{ini})\omega_{ps}(\boldsymbol{\theta}_{Ts} - \boldsymbol{\theta}) \ , \end{aligned} \tag{38}$$

where

$$\mathbf{w}_{ini} = \mathbf{k}_{ini} = \begin{bmatrix} 0.01 & 0.01 & 0.01 & 0.01 & 0.01 & 0.01 \end{bmatrix}. \tag{39}$$

The preset threshold ω_{ps} is 5, *i.e.*, eq.(38) is applied only when the $\omega_{ps} \geq 5$, otherwise, $\mathbf{h}$ still computed

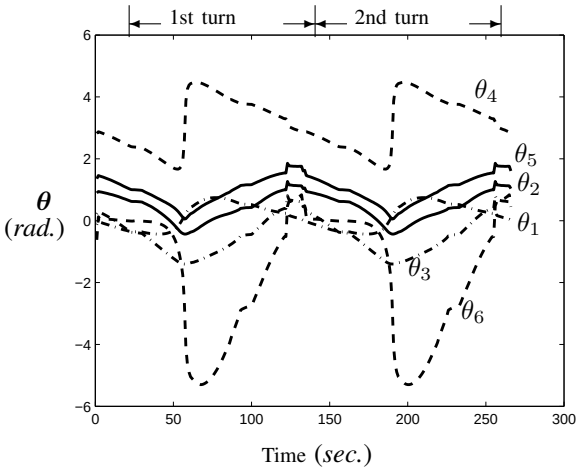

Figure 5. Test I: Joint position with respect to time with the joint-limits avoidance strategy.

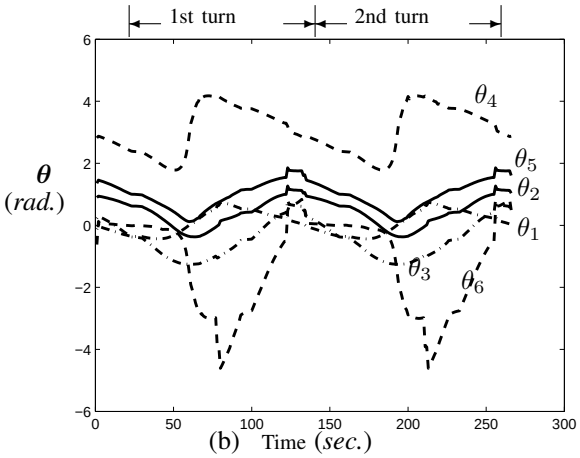

(b)

Figure 6. Test II: Joint position with respect to time with the joint-limits and the singularity avoidance strategy.

by eq.(34). The joint trajectory with TWA considering both joint-limits and singularity avoidance is shown in Figure 6, where the joint motion range is smaller than the result reached in Test I. The closest configuration to singularity appears at instants 64 and 197 second, with the singularity indices of

$$\omega_{cond} = 56, \quad \omega_{mom} = 0.03, \quad \omega_{ps} = 43.2. \tag{40}$$

By comparing Test I and Test II, the maximum value of the condition number ω_{cond} is decreased from 163 to 56, *i.e.*, the shape of the manipulability ellipsoid becomes more spherical. The minimum value of ω_{mom} increases from 0.0066 to 0.03, *i.e.*, the volume of the manipulability ellipsoid increase. The maximum value of ω_{ps} decreases from 156 to 43, *i.e.*, the EE move faster in the direction of the minor axis of the manipulability ellipsoid. As a result

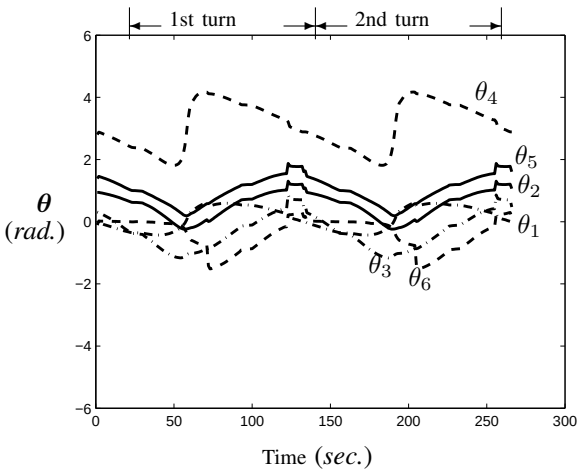

Figure 7. Test III: Joint position with respect to time with joint-limits and singularity avoidant strategy and adapted weighting vectors.

of the increasing of the distance from singularities, the maximum rotation velocity of the fourth joint is lower to 22 deg./s.

5.4. *Test III: Joint-limits and Kinematic Singularity Avoidance with Adapted Weighting Vector*

As mention before, the setting of the weighting vector has great influence on the result. In Test III, the initial weighting vectors are adapted to weighting vectors $\mathbf{w}_{adp}$ and $\mathbf{k}_{adp}$, and are applied into eq.(38).

$$\mathbf{w}_{adp} = \begin{bmatrix} 0.01 & 0.01 & 0.01 & 0.01 & 0.01 & 0.03 \end{bmatrix}, \tag{41}$$

$$\mathbf{k}_{adp} = \begin{bmatrix} 0.01 & 0.01 & 0.01 & 0.01 & 0.01 & 0.05 \end{bmatrix}. \tag{42}$$

The resulting joint trajectory with the adapted weighting vectors is shown as Figure 7, where the motion range of sixth joint is only 33% of the one in Test II. The closest configuration to singularity appears at instant 61 and 194 second, with the singularity indices of

$$\omega_{cond} = 31, \quad \omega_{mom} = 0.076, \quad \omega_{ps} = 20.2. \tag{43}$$

These singularity indices are enhanced almost 100% as comparing to Test II.

Among all the three tests above, the orientation and position errors between the reached and desired path in task space are studied in order to verify the solution accuracy. All these three tests can reach same level of position accuracy, *i.e.*, the maximum position error was 0.0024mm. Relating to the orientation, Tests I and II can reach the same level accuracy, *i.e.*, the

Test	Motion range	Max. ω_{cond}	Min. ω_{mom}	Max. ω_{ps}	Max. J6 velocity	Max. J4 velocity	Error orien.	Error posi.
I	$-5.3 \sim 4.47$	163	0.0066	157	57	74	0.0013	0.0024
II	$-4.6 \sim 4.17$	56	0.03	43.2	56	22	0.0013	0.0024
III	$-1.52 \sim 4.17$	31	0.076	20.2	37	26	0.00077	0.0024
unit	$radian$				$deg./s$	$deg./s$	$radian$	mm

Table 2
Tests comparison, where ω_{cond} is condition number of $\mathbf{J}$, ω_{mom} is the manipulability measure.

maximum norm of orientation error is 0.00128rad. Test III can reach higher orientation accuracy, its orientation error is 0.00077rad.

All these comparison are summarized in Table 2. Obviously, with applying our criterion of eq.(38) in Test II, the distance from singularities is increased while minimizing the the joint motion range; and with adapting the weighting vectors in Test III, a much better solution can be reached.

6. Conclusions

The inverse kinematic solutions that are able to take advantage of the functional redundancy of the welding operation are proposed and studied in this paper. When a welding task is performed with a 6-axis manipulator, the so-called functional redundancy occurs. With the help of this redundancy, it is possible to optimize joint trajectory relative to various performance criterions.

In order to keep the robot configuration as far as possible from singularities, the condition number ω_{cond} and manipulability ω_{mom} are not only used, but also combined to generate a new kinetostatic performance index ω_{ps} which evaluates both the shape and volume of the manipulability ellipsoid.

The welding example compares the optimization results with three tests. The proposed twist decomposition approach, *i.e.*, TWA, with joint-limits and singularity avoidance as the secondary task is able to reach the best solution with this trajectory. Hence, the twist decomposition approach has proven to be able to optimize the joint space trajectory with the different performance criterions.

Acknowledgments

The financial support from NSERC Industrial Postgraduate Scholarship and from Jabez Technologies Inc. are gracefully acknowledged.

References

Angeles, J., Habib, M. and Lopez-Cajun, C.S. (1987), "Efficient Algorithms for the Kinematic Inversion of redundant Robot Manipulators", *Int. J. of Robotics and Automation*, vol. 2, no. 3, pp. 106-115.

Angeles, J. (2003), *Fundamental of Robotic Mechanical Systems: Theory, Methods, and Algorithms*, second edition, Springer-Verlag, New York.

Arenson, N., Angles, J. and Slutski, L. (1998), "Redundancy-resolution algorithms for isotropic robots", *Advances in Robot Kinematics: Analysis and Control*, pp. 425-434, Salzburg.

Baron, L. (2000), "A joint-limits avoidance strategy for arc-welding robots", *Int. Conf. on Integrated Design and Manufacturing in Mech. Eng.*, Montreal, Canada, May 16-19.

Bedrossian, N. (1990), "Classification of singular configurations for redundant manipulators", *IEEE International Conference on Robotics and Automation*, pp. 818-823.

Chaumette, F., Marchand, É. (2001), "A redundancy-based iterative approach for avoiding joint limits: application to visual servoing", *IEEE Trans. on robotics and automation*, vol. 17, no. 5, pp. 719-730.

Huo, L., and Baron, L. (2005), "Kinematic inversion of functionally-redundant serial manipulators: application to arc-welding", *Trans. of the Canadian Society for Mech. Eng.*, vol. 29, no. 4, pp. 679-690.

Klein, C.A. and Huang, C.-H. (1983), "Review of pseudoinverse control for use with kinematically redundant manipulators", *IEEE Trans. on Systems, Man, and Cyb.*, vol. SMC-13, no. 3, pp. 245-250.

Liégeois, A. (1977), "Automatic supervisory control of the configuration and behavior of multibody mechanisms", *IEEE Trans. on System, Man, Cybern.*, vol. SMC-7, no. 12, pp. 245-250.

Marani, G., *et al.* (2002), "A real-time approach for singularity avoidance in resolved motion reate control of robotic manipualtors", *IEEE International Conference on Robotics and Automation*, pp. 1973-1978.

Nakamura, Y., Hanafusa, H. and Yoshikawa, T. (1987), "Task-priority based redundancy control of robot manipulators", *Int. J. Robotics Research*, Vol. 6, No. 2.

Salisbury, J. K. and Craig, J. J. (1982), "Articulated hands, force and kinematic issues", *The Int. J. Robotics* Res. 1, no.1, pp. 4-17.

Samson, C., Le Borgne, M. and Espiau, B. (1991), *Robot control: the task function approach*, Oxford [Angleterre]: Clarendon Press.

Sciavicco, L. and Siciliano, B. (2000), *Modelling and control of robot manipulators*, Springer, London.

Siciliano, B. (1992), "Solving manipulator redundancy with the augmented task space method using the constraint Jacobian transpose", *IEEE Int. Conf. on Robotics and Automation*, vol. 5, pp. 1-8.

Whitney, D.E. (1969), "Resolved motion rate control of manipulators and human prostheses", *IEEE Trans. Man-Machine Syst.*, vol. 10, no. 2, pp. 47-53.

Whitney, D.E. (1972), "The mathematics of coordinated control of prosthetic arms and manipulator", *ASME J. Dynamics Syst., Measur. and Cont.*, vol. 94, no. 4, pp. 303-309.

Yoshikawa, T. (1984), "Analyais and control of robot manipulators with redundancy", *Robotics Research: The First International Symposium*, pp. 735-747.

Yoshikawa, T. (1990), *Foundations of robotics: analysis and control*, The MIT press.

Yoshikawa, T. (1996), "Basic optimization methods of redundant manipulators", *Lab. Robotics and Aut.*, vol. 8, No. 1, pp. 49-60.